

Relaxation time of the global order parameter on multiplex networks: the role of interlayer coupling in Kuramoto oscillators

Alfonso Allen-Perkins^{1,2}, Thiago Albuquerque de Assis^{1,2}, Juan Manuel Pastor¹, Roberto F. S. Andrade^{2*}

¹*Complex System Group, Universidad Politécnica de Madrid, 28040-Madrid, Spain*

²*Instituto de Física, Universidade Federal da Bahia, 40210-210, Salvador, Brazil*

(Dated: October 4, 2018)

Abstract

This work considers the timescales associated with the global order parameter and the interlayer synchronization of coupled Kuramoto oscillators on multiplexes. For the two-layer multiplexes with initially high degree of synchronization in each layer, the difference between the average phases in each layer is analyzed from two different perspectives: the spectral analysis and the non-linear Kuramoto model. Both viewpoints confirm that the prior timescales are inversely proportional to the interlayer coupling strength. Thus, increasing the interlayer coupling always shortens the transient regimes of both the global order parameter and the interlayer synchronization. Surprisingly, the analytical results show that the convergence of the global order parameter is faster than the interlayer synchronization, and the latter is generally faster than the global synchronization of the multiplex. The formalism also outlines the effects of frequencies on the difference between the average phases of each layer, and identifies the conditions for an oscillatory behavior. Computer simulations are in fairly good agreement with the analytical findings and reveal that the timescale of the global order parameter is at least half times smaller than timescale of the multiplex.

*Electronic address: alfonso.allen@hotmail.com; Electronic address: thiagoaa@ufba.br; Electronic address: juanmanuel.pastor@upm.es; Electronic address: randrade@ufba.br

I. INTRODUCTION

The large number of recent investigations on multilayer networks have contributed to uncover several topological and dynamical aspects of complex systems [1–6]. These studies have been motivated by the observation that several such systems can be divided, in a very natural way, into subsets of components that interact in a different way with the co-participants of the same set as compared to members of other subsets. In this way, each such subset can be represented by a layer of multilayer network. This concept has proven to be broad enough to represent different interaction aspects one same agent, provided it also interact differently with members of other subsets [7–9].

Multiplexes form a particular class of multilayer networks, where each layer is formed by the same number N of nodes. Moreover, a multiplex is formed by agents that are identified as one network node, with its own label, in every multiplex layer [9–11]. Because of this, each of these agent’s representation is connected to its own representations in all other layers [12–14]. The strength of these interactions can be dependent of the agent and of the layers between which the interaction occurs [15–17].

These properties make multiplexes a suitable representation of actual complex systems, where each agent has multiple purposes and abilities. This is the case, for instance, of economic systems where each agent represents an investor that can trade in different world markets. It can use the communication flow between markets and different market features expressed by local bylaw restrictions to develop strategies in each market to maximize hedge, risk and profits. Under these circumstances, it is natural to ask how and if cooperation and competition [18–23] favor or not the spread of information and synchronization [24–27] among the different layers.

To help understand real-world complex dynamics, several synchronous models with non-identical interacting agents have been introduced for a description of synchronization, starting from the Rössler and the Kuramoto model [28, 29] in homogeneous structures. More recently, network science explored similar models on non-homogenous structures [25, 30–32]. These dynamic models are sufficiently complex to be non trivial and display a large variety of synchronization patterns. Particularly, the Kuramoto model has the advantage of being sufficiently flexible to be adapted to many different contexts and, at the same time, simple enough to be mathematically tractable [33]. Most of the research done about the Kuramoto

model in complex networks has been summarized in the review of Rodrigues *et al.* [34].

The collective dynamics of several interacting populations of Kuramoto oscillators has been investigated on multilayers [35–37]. Most of the studies on network synchronization focus on effects of network topology on the dynamics in the stationary regime, or when the asymptotic phase of the synchronization is reached. Other investigations have addressed the question of multiplex diffusion [5, 38], and the limits it can be enhanced in comparison to the corresponding spread processes in a single layer. However, once the question of how fast the network synchronizes in the steady state is equally important [34], here we want to focus on the difference between diffusion and synchronization speed in multiplexes. The two phenomena are certainly related but, as we will discuss in the forthcoming sections, they also present different features in the multiplex topology.

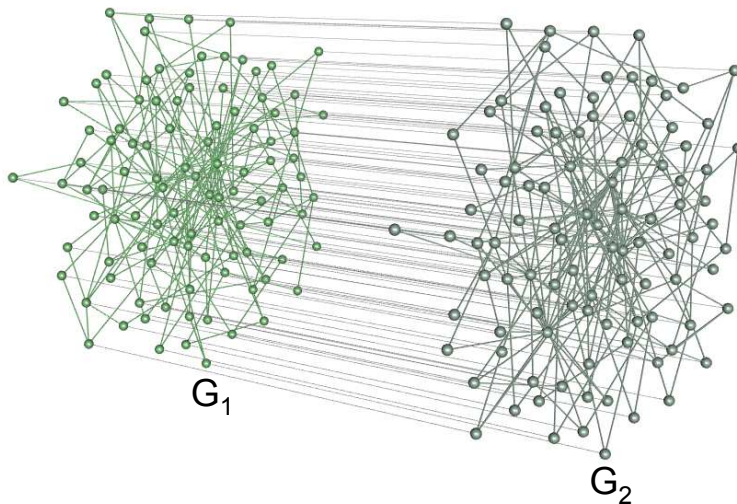


FIG. 1: Example of an undirected multiplex network with two layers, G_1 and G_2 (data visualization with MuxViz [39]).

In this work, we present analytical results for the multiplex order parameter are derived from Kuramoto’s equations of motion, both in the linear approximation and in their complete non-linear form, under the assumption that the initial order parameter of each layer is close to unity. Numerical integration of equations of motion corroborate these predictions and present a consistent scenario where it is possible to identify the diffusion relaxation time and the interlayer synchronization phase. As a consequence, the interlayer synchronization is observed to proceed at a non-smaller pace as compared to diffusion.

The paper is organized as follows. In section II, we define the model and briefly list the main results of the diffusion relaxation time in multiplexes [1, 2, 5, 38, 40]. In section III, the relaxation time of the order parameter and of the interlayer synchronization are deduced from spectral analysis and the non-linear Kuramoto model. Numerical results supporting the analytical expressions are presented in section IV. Section V summarizes our conclusions.

II. KURAMOTO MODEL IN MULTIPLEXES AND DIFFUSION

We consider initially an undirected multiplex \mathcal{M} with M layers G_α , $1 \leq \alpha \leq M$, where each layer contains N nodes identified by x_n^α , $1 \leq n \leq N$ (see Fig. 1). A system of coupled Kuramoto oscillators, which takes into account the intra-layer and inter-layer connections, is defined on \mathcal{M} . The oscillator in each node x_n^α of the layer G_α is characterized by its phase θ_n^α , whose dynamics is described by

$$\dot{\theta}_n^\alpha = \Omega_n^\alpha + \lambda^\alpha \sum_{x_m^\alpha \in G_\alpha} w_{nm}^\alpha \sin(\theta_m^\alpha - \theta_n^\alpha) + \sum_{\substack{\beta=1 \\ \alpha \neq \beta}}^M \lambda^{\alpha\beta} w_{nn}^{\alpha\beta} \sin(\theta_n^\beta - \theta_n^\alpha). \quad (1)$$

Here, Ω_n^α is the natural frequency of the oscillator x_n^α , λ^α and $\lambda^{\alpha\beta}$ are the coupling strength of the layer α and of the interlayer $\alpha\beta$, respectively, w_{nm}^α is the weight of the connection between the nodes x_n^α and x_m^α , and $w_{nn}^{\alpha\beta}$ is the weight of the connection between the nodes x_n^α and x_n^β . In the case of a unweighted and undirected \mathcal{M} , $w_{mn}^{\alpha\beta} = 1$ and $w_{nm}^\alpha = 1$ if there is a link between the nodes x_n^α and x_m^α , and 0 otherwise.

To present a closer comparison between the results for Eq. 1 and those for multiplex diffusion [1, 2, 5, 38, 41, 42], we consider first the most simple case of undirect $M = 2$ multiplex, without sources and sinks of frequency ($\Omega_n^\alpha = 0$), for which the linear approximation of the Kuramoto model reads

$$\dot{\theta}_n^\alpha(t) = \lambda^\alpha \sum_{x_m^\alpha \in G_\alpha} w_{nm}^\alpha (\theta_m^\alpha - \theta_n^\alpha) + \lambda^{12} (\theta_n^\beta - \theta_n^\alpha), \quad (2)$$

with $1 \leq n, m \leq N$, $1 \leq \alpha, \beta \leq 2$ and $w_{nn}^{12} = 1$.

Once Eq. 2 is equivalent to the multiplex diffusion equation [1, 38], it can be written as

$$\dot{\vec{\theta}} = -\mathcal{L}\vec{\theta}, \quad (3)$$

where $\vec{\theta}$ is a column vector that describes the phase of the oscillators such that $\vec{\theta}^T = (\theta_1^1, \dots, \theta_N^1 | \theta_1^2, \dots, \theta_N^2)$, X^T stands for the transpose of matrix X . \mathcal{L} , the *supra-Laplacian matrix* of \mathcal{M} , is defined as

$$\mathcal{L} = \left(\begin{array}{c|c} \lambda^1 \mathbf{L}_1 + \lambda^{12} \mathbf{I} & -\lambda^{12} \mathbf{I} \\ \hline -\lambda^{12} \mathbf{I} & \lambda^2 \mathbf{L}_2 + \lambda^{12} \mathbf{I} \end{array} \right), \quad (4)$$

where \mathbf{I} is a $N \times N$ identity matrix and \mathbf{L}_α is the usual $N \times N$ Laplacian matrix of G_α , with elements $(\mathbf{L}_\alpha)_{nm} = s_n^\alpha \delta_{nm} - w_{nm}^\alpha$. $s_n^\alpha = \sum_{x_m^\alpha \in G_\alpha} w_{nm}^\alpha$ and δ is the Kronecker delta function.

To characterize the eigenvalue spectrum $S(\mathcal{L}) \equiv \{\Lambda_i\}$, we rank its eigenvalues in ascending order $0 = \Lambda_1 < \Lambda_2 \leq \dots \leq \Lambda_{2N}$ [38, 43, 44]. The solution of Eq. 3 in terms of the normal modes $\varphi_i(t)$ is given by

$$\vec{\varphi} = \mathbf{B}^T \vec{\theta}, \quad (5)$$

where $\varphi_i(t) = \varphi_i(0)e^{-\Lambda_i t}$, and $\mathbf{B} = (\vec{v}_1 | \vec{v}_2 | \dots | \vec{v}_{2N})$ is the matrix of eigenvectors of \mathcal{L} (i.e. $\Lambda_i \vec{v}_i = \mathcal{L} \vec{v}_i$) [38, 43, 44].

Consequently, the diffusive relaxation time of multiplex networks, $\tau_{\mathcal{M}}$, depends on the network topology and is dominated by the smallest nonzero eigenvalue Λ_2 of the \mathcal{L} , i.e. $\tau_{\mathcal{M}} = 1/\Lambda_2$ [5, 38, 40]. This behavior is in line with analogous findings for mono-layer networks of coupled Kuramoto oscillators, which have shown that the relaxation time mainly depends on the smallest nonzero eigenvalue of the corresponding Laplacian matrix [45–48].

If we consider $\lambda^1 = \lambda^2 = 1$, the analytical results in [5, 38] for multiplex diffusion indicate the following properties of $S(\mathcal{L})$:

- (i) $2\lambda^{12}$ is always an eigenvalue of \mathcal{L} .
- (ii) When the interlayer coupling is small, i.e. $\lambda^{12} \ll 1$, $\Lambda_2 = 2\lambda^{12}$.
- (iii) When the interlayer coupling is large, i.e. $\lambda^{12} \gg 1$, $\Lambda_2 \sim \sigma_s/2$, where σ_s is the smallest nonzero eigenvalue of the superposition matrix $(L_1 + L_2)/2$, and L_α is the Laplacian matrix of layer α .

In Fig. 2 we show an example of the dependence of Λ_2 on λ^{12} .

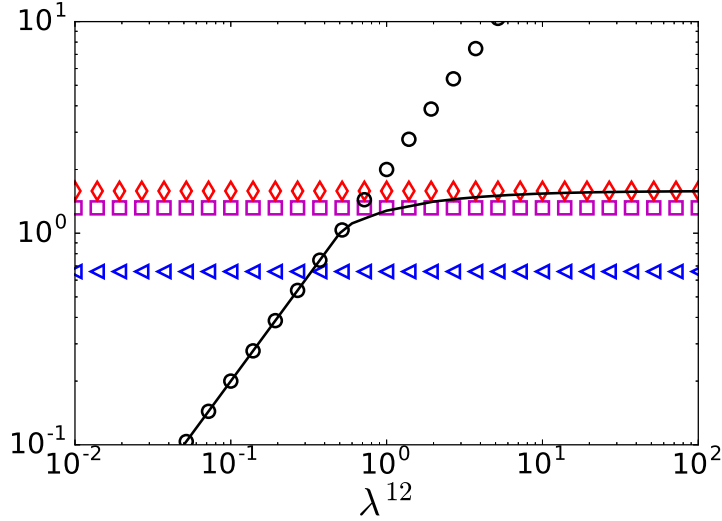


FIG. 2: Dependence on λ^{12} of the second nonzero smallest eigenvalues σ_2 of the Laplacian matrices of layer 1 (blue triangles), layer 2 (magenta squares), the superposition of both layers (red rhombus), Λ_Δ (black circles) and Λ_2 (black continuous line). The results are presented for a $M = 2$ multiplex \mathcal{M} with $N = 100$ nodes in each layer, when $\lambda^1 = \lambda^2 = 1$.

Each layer consists of scale-free network with degree distribution $P(k) \sim k^{-3}$.

III. RELAXATION TIME OF KURAMOTO ORDER PARAMETER

The level of synchronization in a general system \mathcal{S} of \mathcal{N} Kuramoto oscillators is described by a parameter r defined as

$$r(t)e^{i\psi(t)} = \frac{1}{\mathcal{N}} \sum_{x_n^\alpha \in \mathcal{S}} e^{i\theta_n^\alpha(t)} \rightarrow r(t) = \frac{1}{2N} \left| \sum_{x_n^\alpha \in \mathcal{M}} e^{i\theta_n^\alpha(t)} \right|, \quad (6)$$

where $\psi(t)$ is the average phase of the oscillators in the system. Here, $r \approx 1$ ($r \approx 0$) indicates a full synchronization (an asynchronous behavior) of the system \mathcal{M} [28, 29].

In this work, Eq.(6) is used to both layer (r_α) and global (r) order parameters, by appropriately choosing the set of nodes (G_α or the whole set \mathcal{M}) where the sum is performed. $\psi^\alpha(t)$ and $\psi(t)$ indicate α -layer and multiplex average phases, respectively. When $M = 2$, it is straightforward to express r in terms r_α as

$$r e^{i\psi} e^{-i\psi^2} = \frac{r_1 e^{i\psi^1} + r_2 e^{i\psi^2}}{2} e^{-i\psi^2} \rightarrow r = \sqrt{\frac{r_1^2 + r_2^2 + 2r_1 r_2 \cos(\psi^1 - \psi^2)}{4}}. \quad (7)$$

For the purpose of putting forward the analytical results, we restrict our analysis to the

$r_\alpha(t) \approx 1$ case, i.e, we assume that $\theta_n^\alpha(t) \approx \psi^\alpha(t)$ for $1 \leq n \leq N_\alpha$, $1 \leq \alpha \leq M$, $\forall t$. In section IV we show that these conditions are fairly well satisfied for the system in Eq. 1 when, at $t = 0$, the degree of synchronization in each layer is high. Under such restrictions, we rewrite r for the $M = 2$ case as

$$r(t) \approx \left| \cos \left(\frac{\psi^1 - \psi^2}{2} \right) \right| = \left| \cos \left(\frac{\Delta}{2} \right) \right|, \quad (8)$$

where $\Delta(t) = \psi^1(t) - \psi^2(t)$ is the difference between the average phases of the layers G_1 and G_2 . Hence, the timescales of r and $\left| \cos \left(\frac{\psi^1 - \psi^2}{2} \right) \right|$ are the same.

The linear relaxation time of the interlayer synchronization process can be estimated by the difference between the average phases of layers G_1 and G_2 , Δ , defined in Eq. 8. Taking into account the property (i) of $S(\mathcal{L})$, we define $\Lambda_\Delta \equiv 2\lambda^{12}$. Its column eigenvector \vec{v}_Δ is such that $\vec{v}_\Delta^T = \left(v_1^1, \dots, v_N^1 \mid v_1^2, \dots, v_N^2 \right) = \left(1, \dots, 1 \mid -1, \dots, -1 \right)$.

By definition \mathbf{L}_1 and \mathbf{L}_2 are symmetric real matrices with row and column sums zero, i.e. $\mathbf{L}_\alpha \vec{1} = \vec{0}$, where \vec{x} is an all-x vector. Thus,

$$\mathcal{L} \vec{v}_\Delta = \left(\begin{array}{c|c} \lambda^1 \mathbf{L}_1 & \mathbf{0} \\ \hline \mathbf{0} & \lambda^2 \mathbf{L}_2 \end{array} \right) \vec{v}_\Delta + \left(\begin{array}{c|c} \lambda^{12} \mathbf{I} & -\lambda^{12} \mathbf{I} \\ \hline -\lambda^{12} \mathbf{I} & \lambda^{12} \mathbf{I} \end{array} \right) \vec{v}_\Delta = \vec{0} + 2\lambda^{12} \vec{v}_\Delta = \Lambda_\Delta \vec{v}_\Delta. \quad (9)$$

Following [38, 43, 44], the normal mode related to $\Lambda_\Delta = 2\lambda^{12}$ is

$$\vec{v}_\Delta^T \vec{\theta} = \sum_{x_n^1 \in G_1} \theta_n^1 - \sum_{x_m^2 \in G_2} \theta_m^2 = \varphi_\Delta(0) e^{-\Lambda_\Delta t}. \quad (10)$$

According to Eq. 8, when the assumption $r_\alpha(t) \approx 1$ is valid, Eq. 10 leads to

$$\Delta(t) = \psi^1(t) - \psi^2(t) \approx \frac{\varphi_\Delta(0)}{N} e^{-\Lambda_\Delta t}. \quad (11)$$

Since the relaxation time for interlayer synchronization can be estimated by $\tau_\Delta = 1/\Lambda_\Delta$, we draw the following similar conclusions to the results listed in section II:

- (i) When $\lambda^{12} \ll 1$, the diffusive timescale of \mathcal{M} coincides with the interlayer synchronization time, i.e. $\Lambda_2 = \Lambda_\Delta$.
- (ii) When $\lambda^{12} \gg 1$, the diffusive timescale of \mathcal{M} exceeds the interlayer synchronization time, i.e. $\Lambda_2 \ll \Lambda_\Delta$ ($\Leftrightarrow \tau_{\mathcal{M}} \gg \tau_\Delta$).

To derive the non-linear relaxation timescale of the interlayer synchronization for the system in Eq. 1, we rewrite it in terms of the order parameters r_α of each layer G_α as

$$\dot{\theta}_n^\alpha = \Omega_n^\alpha + \lambda^\alpha r_\alpha N \bar{w}_n^\alpha \sin(\psi^\alpha - \theta_n^\alpha) + \sum_{\substack{\beta=1 \\ \alpha \neq \beta}}^M \lambda^{\alpha\beta} w_{nn}^{\alpha\beta} \sin(\theta_n^\beta - \theta_n^\alpha), \quad (12)$$

where \bar{w}_n^α is defined by

$$\bar{w}_n^\alpha \sum_{x_m^\alpha \in G_\alpha} e^{i\theta_m^\alpha} = \sum_{x_m^\alpha \in G_\alpha} w_{nm}^\alpha e^{i\theta_m^\alpha}. \quad (13)$$

As $r_\alpha(t) \approx 1$, we obtain the following approximation for an undirected multiplex \mathcal{M} :

$$\begin{aligned} \dot{\psi}^\alpha &= \frac{1}{N} \sum_{x_n^\alpha \in G_\alpha} \dot{\theta}_n^\alpha = \frac{1}{N} \left[\sum_{n=1}^N \Omega_n^\alpha \right] + \sum_{\substack{\beta=1 \\ \alpha \neq \beta}}^M \lambda^{\alpha\beta} \sin(\psi^\beta - \psi^\alpha) \left[\sum_{n=1}^N w_{nn}^{\alpha\beta} \right] = \\ &= \langle \Omega \rangle_\alpha + \sum_{\substack{\beta=1 \\ \alpha \neq \beta}}^M \lambda^{\alpha\beta} \sin(\psi^\beta - \psi^\alpha) \frac{s^{\alpha\beta}}{N}, \end{aligned} \quad (14)$$

where $s^{\alpha\beta}$ is the sum of the interlayer strengths between nodes of the layers G_α and G_β . Also, the evolution of the average phase difference between G_α and G_β becomes

$$\begin{aligned} \dot{\Delta}^{\alpha\beta} &= \dot{\psi}^\alpha - \dot{\psi}^\beta = \left(\langle \Omega \rangle_\alpha - \langle \Omega \rangle_\beta \right) - 2\lambda^{\alpha\beta} \sin(\psi^\alpha - \psi^\beta) \frac{s^{\alpha\beta}}{N} \\ &+ \sum_{\substack{\gamma=1 \\ \gamma \neq \alpha, \beta}}^M \left[\lambda^{\alpha\gamma} \sin(\psi^\gamma - \psi^\alpha) \frac{s^{\alpha\gamma}}{N} - \lambda^{\beta\gamma} \sin(\psi^\gamma - \psi^\beta) \frac{s^{\beta\gamma}}{N} \right]. \end{aligned} \quad (15)$$

Restricting the discussion to $M = 2$ and $w_{nn}^{12} = 1 \Rightarrow s^{12} = N$, we consider first $\langle \Omega \rangle_1 \approx \langle \Omega \rangle_2$, so that the synchronization of the system can be estimated as

$$\eta_\Delta(t) \equiv \left| \tan \left(\frac{\Delta(t)}{2} \right) \right| = \left| \tan \left(\frac{\Delta(0)}{2} \right) \right| e^{-\int_0^t 2\lambda^{12} dt'} = \left| \tan \left(\frac{\Delta(0)}{2} \right) \right| e^{-\Lambda_\Delta t}, \quad (16)$$

where we use the short-hand notation $\Delta(t) = \Delta^{12}(t)$. Eq. 16 and the series expansion $\tan(x) \simeq x$ show that the relaxation time of Δ is dominated by Λ_Δ , i.e., $\Delta/2 \propto e^{-\Lambda_\Delta t}$.

Next, if $\langle \Omega \rangle_1 \neq \langle \Omega \rangle_2$, it is possible to integrate Eq. 15 and express the corresponding solution in terms of a variable $\xi(t)$ such that

$$\xi(t) = \frac{\left| \tan\left(\frac{\Delta(t)}{2}\right) - \text{sgn}(\langle\Omega\rangle^{12}) (|R| - \sqrt{R^2 - 1}) \right|}{\left| \tan\left(\frac{\Delta(t)}{2}\right) - \text{sgn}(\langle\Omega\rangle^{12}) (|R| + \sqrt{R^2 - 1}) \right|} = \xi(0)e^{-t|\langle\Omega\rangle^{12}|\sqrt{R^2-1}}, \quad (17)$$

where $\text{sgn}(\cdot)$ is the sign function, $\langle\Omega\rangle^{12} \equiv \langle\Omega\rangle_1 - \langle\Omega\rangle_2$ and

$$R = \frac{\Lambda_\Delta}{\langle\Omega\rangle_1 - \langle\Omega\rangle_2} \equiv \frac{\Lambda_\Delta}{\langle\Omega\rangle^{12}}. \quad (18)$$

Eq. 17 is valid when $|R| > 1$ while, for the $|R| \leq 1$, the integration of Eq. 15 results in

$$\tan\left(\frac{\Delta(t)}{2}\right) = R + \sqrt{1 - R^2} \tan\left(\frac{\langle\Omega\rangle^{12} \sqrt{1 - R^2}}{2} t + \tan^{-1}\left(\frac{\tan\left(\frac{\Delta(0)}{2}\right) - R}{\sqrt{1 - R^2}}\right)\right). \quad (19)$$

As can be observed, Eq. 19 shows that $\tan\left(\frac{\Delta(t)}{2}\right)$ is a periodic function for $\Lambda_\Delta \leq |\langle\Omega\rangle^{12}|$. This drifting behavior just states that, if the interlayer coupling strength is not large enough, it is no longer possible to reduce the difference of average frequencies between the layers and entrain the whole system.

Supposing that $\Delta/2 \gtrsim 0$, $\tan\left(\frac{\Delta(t)}{2}\right) \geq 2|R|$ and $\Lambda_\Delta \gg |\langle\Omega\rangle^{12}|$, the absolute value signs in Eq. 17 can be removed and, thus, it can be approximated as:

$$\frac{\tan\left(\frac{\Delta}{2}\right)}{\tan\left(\frac{\Delta}{2}\right) - A} = -\frac{1}{A} \left(\frac{\Delta}{2}\right) - \frac{1}{A^2} \left(\frac{\Delta}{2}\right)^2 - \frac{(A^2 + 3)}{3A^3} \left(\frac{\Delta}{2}\right)^3 - \dots \approx \xi(0)e^{-\Lambda_\Delta t}, \quad (20)$$

where $A = 2|R|\text{sgn}(\langle\Omega\rangle^{12})$. Under these conditions, the relaxation time of Δ is dominated once again by Λ_Δ . Hence, provided that $r_1(t) \approx r_2(t) \approx 1$ and $\Lambda_\Delta \gg |\langle\Omega\rangle^{12}|$, the non-linear Kuramoto model (Eq. 1) and the spectral analysis (see subsection III) lead to the same relaxation time for the interlayer synchronization process for $M = 2$: $\tau_\Delta = 1/\Lambda_\Delta = 1/2\lambda^{12}$.

For small values of Δ , the time evolution of the order parameter in Eq. 8 can be approximated by $r(t) \simeq 1 - \Delta^2/8$. Therefore, the timescale of the order parameter (τ_r) is determined by the smallest nonzero power of $\Delta/2$, and a rough estimation is $\tau_r \gtrsim 1/2\Lambda_\Delta$.

Summarizing the results in sections II and III, the asymptotic synchronization phase of the Kuramoto model on multiplexes is characterized by the following behavior:

- (i) When $\lambda^{12} \ll \lambda^1 = \lambda^2$, the timescales rank as follows: $\tau_{\mathcal{M}} = \tau_\Delta > \tau_r$.
- (ii) When $\lambda^{12} \gg \lambda^1 = \lambda^2$, the timescales rank as follows: $\tau_{\mathcal{M}} \gg \tau_\Delta > \tau_r$.

According to Eq. 16, increasing the value of λ^{12} accelerates the transient regimes of the interlayer synchronization and of the global order parameter, respectively. Additionally, it reduces the difference between the average phase of each layer and, hence, it favors the full synchronization of the system. The important aspect of this result is that, contrary to what is observed for the multiplex diffusive relaxation, when $r_\alpha \simeq 1$.

These results are in accordance with the prior findings on *superdiffusion* [5, 38, 40]. Superdiffusion emerges when the timescale of the multiplex is faster than that of both layers acting separately [5, 38], i.e. $\Lambda_2 > \max(\sigma_2^1, \sigma_2^2)$, where σ_2^α is the smallest nonzero eigenvalue of the Laplacian matrix of layer G_α . For large coupling between layers, spectral analysis predicts that superdiffusion is not guaranteed; it depends on the specific structures coupled together. Increasing the interlayer coupling accelerates the convergence of the global order parameter and of the difference between the average phase of each layer. Nevertheless, it also increases the magnitude of the perturbations that are transmitted across the interlayer.

IV. NUMERICAL RESULTS

In this section we show that the prior analytical findings are in complete agreement with computer simulations. We compare results of the numerical integration of the coupled Kuramoto oscillators for several multiplexes realizations, using 16 digit variables. From the solution for $\theta_n^\alpha(t)$ we obtain the time evolution of $\tan\left(\frac{\Delta(t)}{2}\right)$ and $1 - r(t)$ for the linear and non-linear regimes that are compared, respectively, to

$$\begin{aligned}\eta_2(t) &= \left| \tan\left(\frac{\Delta(0)}{2}\right) \right| e^{-\Lambda_2 t}, \\ \eta_r(t) &= (1 - r(0)) e^{-2\Lambda_\Delta t}.\end{aligned}\tag{21}$$

$\eta_r(t)$ is a measure of the synchronization dynamics, while $\eta_2(t)$ has the same dependence on time as the multiplex diffusive dynamics. Besides that, $\tan\left(\frac{\Delta(t)}{2}\right)$ is also compared to $\eta_\Delta(t)$ in Eq. 16.

Other examples for different values of the interlayer and intralayer coupling constants and several initial conditions for the coupled Kuramoto oscillators, are presented in the Supplementary Material to this paper. All of them are in complete agreement with the results described in this section.

A. Linear Kuramoto model

We start by presenting numerical results from the integration of Eq. 2, where the initial phases $\theta_n^\alpha(0)$ are drawn randomly from a uniform distribution $\mathcal{U}_{\theta^\alpha}(\mu_\alpha - a, \mu_\alpha + a)$, and μ_α is the expected value of θ_n^α . Results satisfying $a \ll 1$ can be compared to the analytical expressions derived in the previous sections for $\tan\left(\frac{\Delta}{2}\right)$ and $1 - r$, as in these cases the condition $r_\alpha \simeq 1$ is satisfied. For the sake of an easier comparison with the analytical results, we set $\lambda^1 = \lambda^2 = \lambda$. We remark that results depend on the following factors: coupling strengths, initial conditions and network topology.

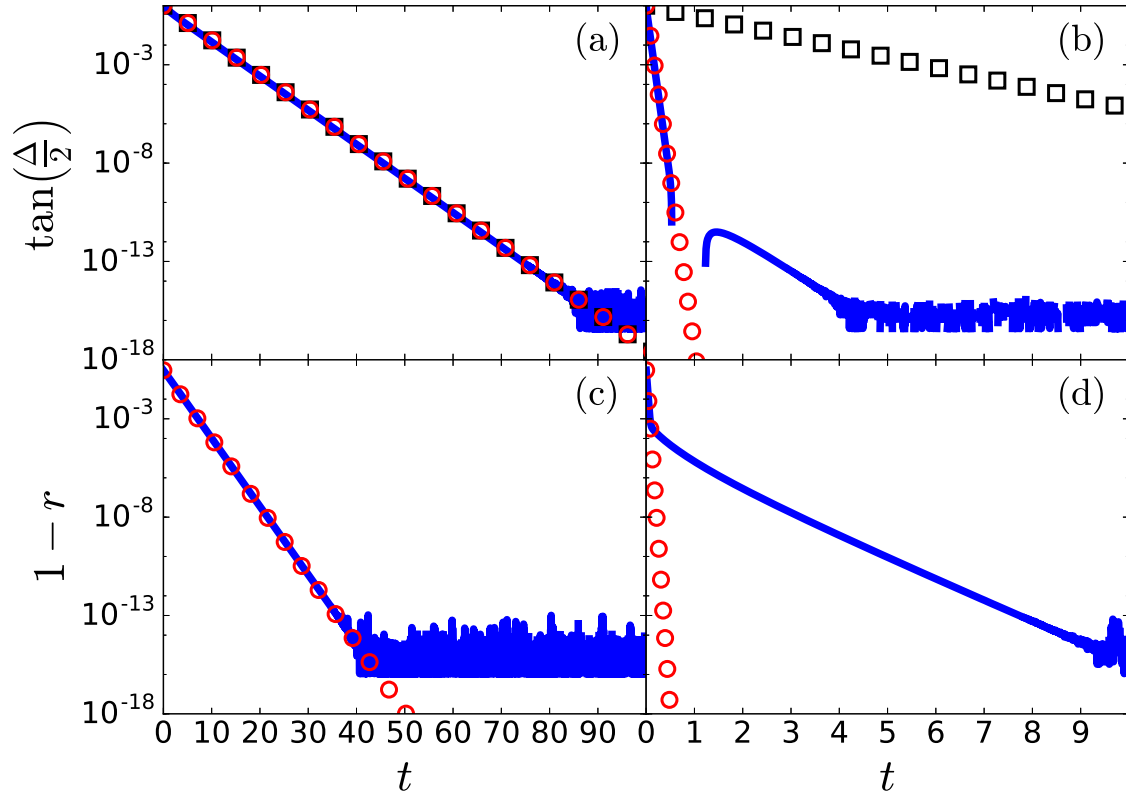


FIG. 3: Numerical results for $N = 500$, $\lambda = 2.0$, $\mu_1 = \pi/2$, $\mu_2 = 0$, and $a = 0.1$. Each multiplex layer has the same topological features described in Fig. 2. Panels (a) and (b): Time evolution of $\tan\left(\frac{\Delta(t)}{2}\right)$ (blue continuous line), $\eta_\Delta(t)$ (red circles) and $\eta_2(t)$ (black squares) for $\lambda^{12} = 0.1\lambda$ (a), and $\lambda^{12} = 10.0\lambda$ (b). Panels (c) and (d): Time evolution of $1 - r(t)$ (blue continuous line) and $\eta_r(t)$ (red circles) for $\lambda^{12} = 0.1\lambda$ (c), and $\lambda^{12} = 10.0\lambda$ (d).

Dependence on coupling strengths is in agreement with section III. Fig. 3a shows that, for $\lambda^{12} \ll \lambda$, the timescales of interlayer synchronization and of diffusion on \mathcal{M} are equal: the time evolution of $\tan\left(\frac{\Delta(t)}{2}\right)$ is well approximated by $\eta_{\Delta}(t)$ and $\eta_2(t)$, i.e. $\Lambda_2 \approx \Lambda_{\Delta}$. However, when $\lambda^{12} \gg \lambda$, these timescales differ, i.e. $\Lambda_2 \neq \Lambda_{\Delta}$, as indicated by lines with different slopes in Fig. 3b. Moreover, it is also shown that the agreement between $\tan\left(\frac{\Delta(t)}{2}\right)$ and $\eta_{\Delta}(t)$ has a lower limit $\sim 10^{-10}$. Nevertheless, the difference between the average phases of both layers relaxes faster than the whole system, i.e. $\tau_{\mathcal{M}} \gg \tau_{\Delta}$ for $\lambda \ll \lambda^{12}$. Both panels reveal the presence of random fluctuations $\sim 10^{-15}$, which depend on precision of the used variables.

The same (somewhat different) features are observed in Figs. 3c (Fig. 3d), where we compare the approximation $\eta_r(t)$ with the actual value of $1 - r(t)$. The evolution of $1 - r(t)$ is well adjusted by $\eta_r(t)$ for $\lambda^{12} \ll \lambda$. However, when $\lambda^{12} \gg \lambda$, the quantities agree with each other in a more limited range $\gtrsim 10^{-4}$.

For a given choice of the coupling parameters, the deviations from the exponential behavior can be influenced by topological differences among the layers and by the initial values $\theta_n^{\alpha}(0)$. To emphasize the importance of the later, we consider $M = 2$ multiplexes where each layer consists of a complete graph, for which analytical expressions for Λ_2 can be obtained (see Appendix). In Fig. 4 we show the numerical results for $1 - r(t)$ when $a = 0$ and 0.1. The inset shows that the time evolution of $1 - r(t)$ is well adjusted by $\eta_r(t)$, when $a = 0$, while departures from the exponential decay take place when $a > 0$. Here, the agreement between the curves is limited to the range $\gtrsim 10^{-6}$.

Fig. 3 and Fig. 4 suggest that it may be possible to relate the range of values of $1 - r$ where the numerical results coincide with the analytical predictions to τ_D , the characteristic timescale for the emergence of these discrepancies. It turns out that τ_D is mainly controlled by the value of Λ_2 as follows:

$$\tau_D \approx \frac{1}{2\Lambda_2}. \quad (22)$$

Therefore, in case $\Lambda_{\Delta} \approx \Lambda_2$, deviations disappear until the numeric precision of the used variables is reached, whether or not $a = 0$ (see Fig. 3a and Fig. 3c). However, if $\Lambda_{\Delta} > \Lambda_2$ and $a > 0$, discrepancies will manifest.

Finally, still using complete graphs for the sake of comparison to analytical expressions, we illustrate the dependence of the multiplex dynamics on the topology, for a given choice

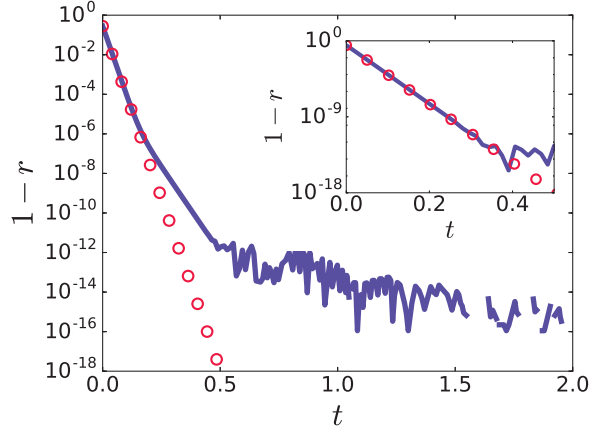


FIG. 4: Time evolution of $1 - r(t)$ (blue continuous line) and $\eta_r(t)$ (red circles) for $N = 10$, $\lambda = 2.0$, $\lambda^{12} = 10\lambda$, $\mu_1 = \pi/2$, $\mu_2 = 0$ and $a = 0.1$. Each layer contains a complete graph.

The inset shows the results by considering $a = 0$.

of the coupling strengths and the initial conditions. We note that the dependence on the topology can be observed just by changing the number of nodes in each layer of complete graph. Indeed, if $\Lambda_\Delta > \Lambda_2$, the smallest nonzero eigenvalue of the supra-Laplacian matrix is $\Lambda_2 = \lambda N$ (see Appendix). Therefore, according to Eq. 22, the smaller the number of nodes N , the larger the deviations, for $\tau_M > \tau_\Delta$ and $a > 0$. In Fig. 5a and Fig. 5b we display the time evolution of $1 - r(t)$, $\eta_r(t)$, and a guide for the eye proportional to $e^{-2\lambda N t}$ for $N = 10$ and $N = 100$, respectively, and $a > 0$. As can be observed, these results are in good agreement with Eq. 22. In the Appendix, we show analytically the dependence of the global order parameter r on $e^{-2\Lambda_2 t}$ (i.e. $e^{-2\lambda N t}$), when each layer of the multiplex network is a complete graph.

B. Non-linear Kuramoto model

The numerical results for the non-linear equations Eq. 1 were obtained using the same procedure described in previous subsection. When all natural frequencies of the oscillators are set to zero, i.e. $\Omega_n^\alpha = 0 \forall n$, the time evolution of $\tan\left(\frac{\Delta(t)}{2}\right)$ and $1 - r(t)$ for $\lambda^{12} \ll \lambda$ are essentially the same as those in Fig. 3a and Fig. 3c. However, when $\lambda^{12} \gg \lambda$, which causes $\Lambda_2 \neq \Lambda_\Delta$ and $\tau_M \gg \tau_\Delta$, $\tan\left(\frac{\Delta(t)}{2}\right)$ deviates both from $\eta_2(t)$ and $\eta_\Delta(t)$ as well as

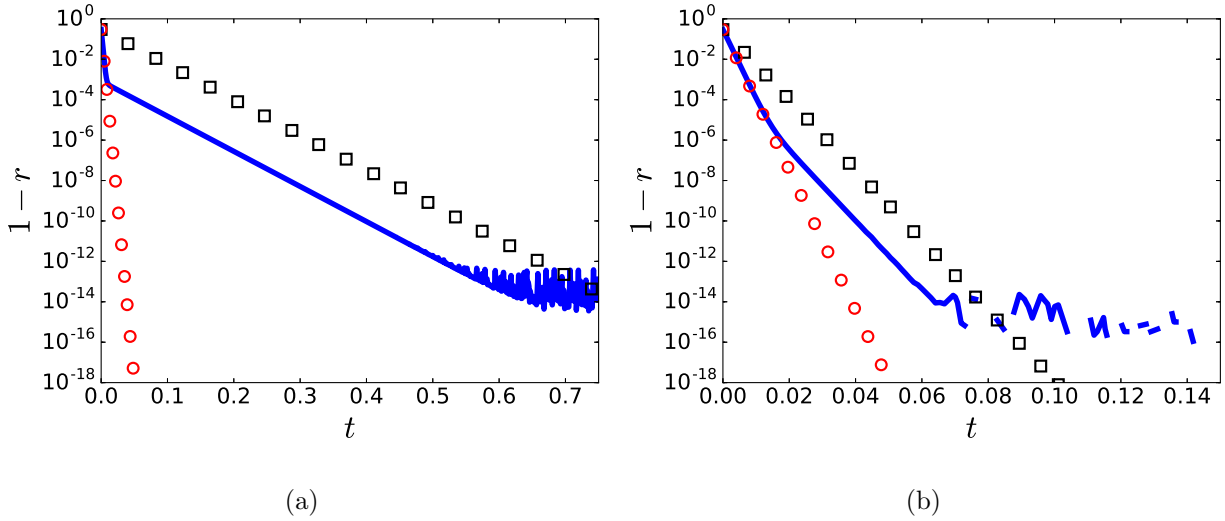


FIG. 5: Time evolution of $1 - r(t)$ (blue continuous line), $\eta_r(t)$ (red circles) and a guide for the eye proportional to $e^{-2\lambda Nt}$ (black squares), for $\lambda = 2.0$, $\lambda^{12} = 100\lambda$, $\mu_1 = \pi/2$, $\mu_2 = 0$ and $a = 0.1$. Each layer contains a complete graph. (a) Left panel: $N = 10$ (b) Right panel: $N = 100$.

$1 - r(t)$ deviates from $\eta_r(t)$. The comparison between Fig. 3b and Fig. 6a shows that the non-linear terms affects the evolution $\tan\left(\frac{\Delta(t)}{2}\right)$. Notice that the effect on the evolution of $1 - r(t) \sim \Delta^2$ is much smaller, in such a way that the changes induced by the non-linear terms in Fig. 6b are minute in comparison to Fig. 3d.

Dependence of $1 - r(t)$ on a for $M = 2$ multiplexes formed by complete graphs is very similar to that in Fig. 4. When $a = 0$, $1 - r(t)$ and $\eta_r(t)$ are in complete agreement, if they are greater or similar to 10^{-12} ; while for $a = 0.1$ deviations appear when $\eta_r(t) \lesssim 10^{-5}$.

Let us now discuss the results when the natural frequencies Ω_n^α are different from zero so that, in general, $\langle\Omega\rangle_1 \neq \langle\Omega\rangle_2$. Following [49], the values of the frequencies are drawn randomly from a uniform distribution $\mathcal{U}(0.8, 1.2)$. As observed in Fig. 7a and Fig. 7b, the time evolution of $\tan\left(\frac{\Delta(t)}{2}\right)$ diverges from $\eta_\Delta(t)$ when $\langle\Omega\rangle_1 \neq \langle\Omega\rangle_2$, for both $\lambda^{12} \ll \lambda$ and $\lambda^{12} \gg \lambda$. In both cases Δ converges to a non-zero value and, consequently, the oscillators do not reach a full synchronization in accordance to Eq. 17 and Eq. 18. We notice that the deviations from the exponential predictions for $\lambda^{12} \ll \lambda$ occur at a larger value of $\eta_2(t)$ as compared to $\lambda^{12} \gg \lambda$. This stays in opposition to the previously observed behavior for $\Omega_n^\alpha \equiv 0$. Indeed, a relatively small interlayer coupling favors the emergence of the deviations,

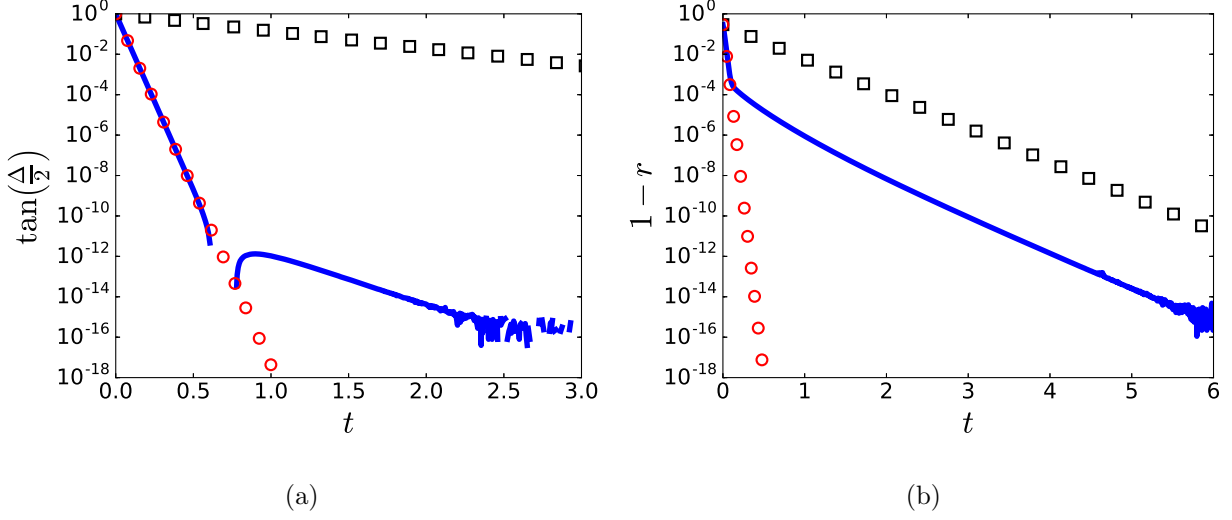


FIG. 6: (a) Left panel: Time evolution of $\tan\left(\frac{\Delta(t)}{2}\right)$, $\eta_\Delta(t)$, and $\eta_2(t)$. (b) Right panel: Time evolution of $1 - r(t)$ and $\eta_r(t)$. $\lambda^{12} = 10.0\lambda$ in both panels, and the used symbols and lines are the same as in Fig. 3b and Fig. 3d. The multiplexes are the same as those used in Fig. 3.

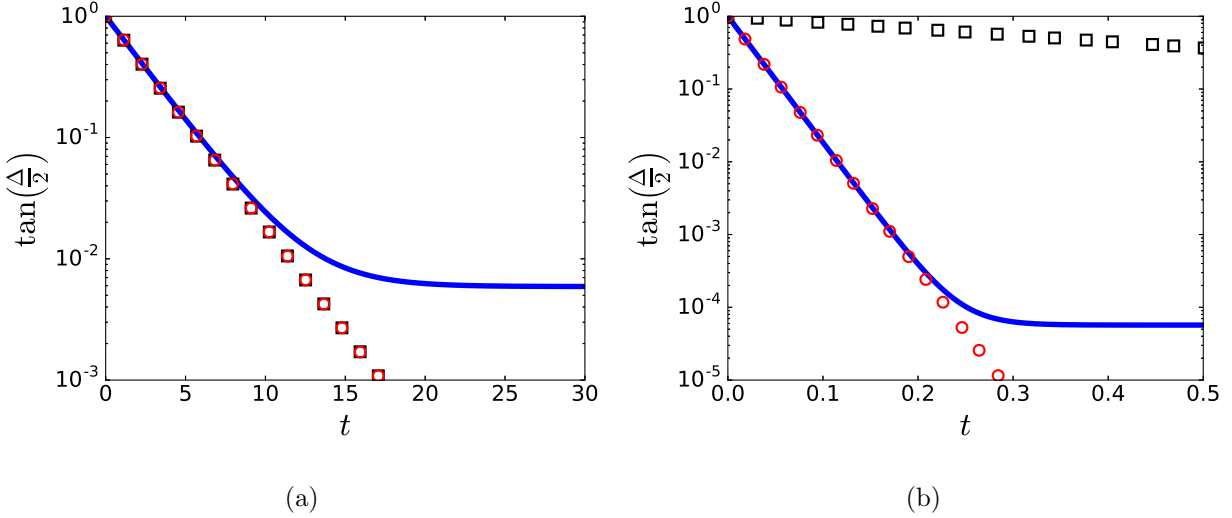


FIG. 7: Time evolution of $\tan\left(\frac{\Delta(t)}{2}\right)$, $\eta_\Delta(t)$, and $\eta_2(t)$. The multiplex parameters, symbols and lines are the same as in Fig. 3a and Fig. 3b, except for $\Omega_n^\alpha \in \mathcal{U}(0.8, 1.2)$. (a) Left panel: $\lambda^{12} = 0.1\lambda$ (b) Right panel: $\lambda^{12} = 10.0\lambda$.

once interlayer synchronization is impeded for $\lambda^{12} \approx 0$. Hence, if $|\langle \Omega \rangle^{12}| > 0$ and $\lambda^{12} \approx 0$, the exponential decay barely takes place. In the case of $\lambda^{12} \gg 0$, the relaxation time of the

synchronization error gets closer to the estimation given by $\eta_r(t)$, whether or not $\lambda \gg \lambda^{12}$.

The asymptotic value of the difference between the average phases of both layers can be estimated from Eq. 17. If $\tan\left(\frac{\Delta(t)}{2}\right) \geq \text{sgn}(\langle\Omega\rangle^{12}) (|R| + \sqrt{R^2 - 1})$, Eq. 17 can be rewritten as

$$\tan\left(\frac{\Delta(t)}{2}\right) = \left(|R| - \sqrt{R^2 - 1} \frac{1 + \xi(0)e^{-t|\langle\Omega\rangle^{12}|\sqrt{R^2-1}}}{1 - \xi(0)e^{-t|\langle\Omega\rangle^{12}|\sqrt{R^2-1}}}\right) \text{sgn}(\langle\Omega\rangle^{12}), \quad (23)$$

so that its asymptotic value $t \rightarrow \infty$ is given by

$$\lim_{t \rightarrow \infty} \tan\left(\frac{\Delta(t)}{2}\right) = (|R| - \sqrt{R^2 - 1}) \text{sgn}(\langle\Omega\rangle^{12}). \quad (24)$$

If $\langle\Omega\rangle_1 \simeq \langle\Omega\rangle_2$, R diverges and Δ decays to zero exponentially. On the other hand, in Fig. 8 we expose the time evolution of $\tan\left(\frac{\Delta(t)}{2}\right)$ for $2\langle\Omega\rangle^{12} = \Lambda_\Delta$. In that case, according to Eq. 17 and Eq. 24, the asymptotic value of the difference between the average phases of both layers is $\psi^1 - \psi^2 = \pi/6$ (green triangles). It is easy to see that the prior estimation is very accurate.

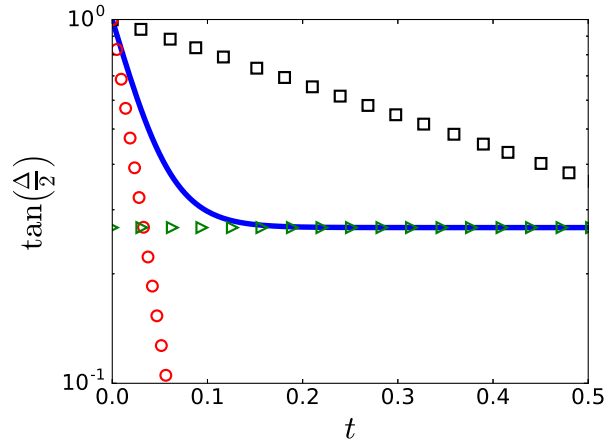


FIG. 8: Time evolution of $\tan\left(\frac{\Delta(t)}{2}\right)$, $\eta_\Delta(t)$, and $\eta_2(t)$. The multiplex parameters, symbols and lines are the same as in Fig. 3b. The model parameters are $\lambda = 2.0$, $\lambda^{12} = 10\lambda$ and $2\langle\Omega\rangle^{12} = \Lambda_\Delta$. Green triangles indicate the asymptotic value obtained with Eq. 17.

Fig. 9a and Fig. 9b illustrate the behavior of $1 - r(t)$ for small and large interlayer coupling, respectively. As can be observed, synchronization error departs from $\eta_r(t)$ values whether or not $\lambda^{12} \ll \lambda$. As expected, its asymptotic value does not decay to zero.

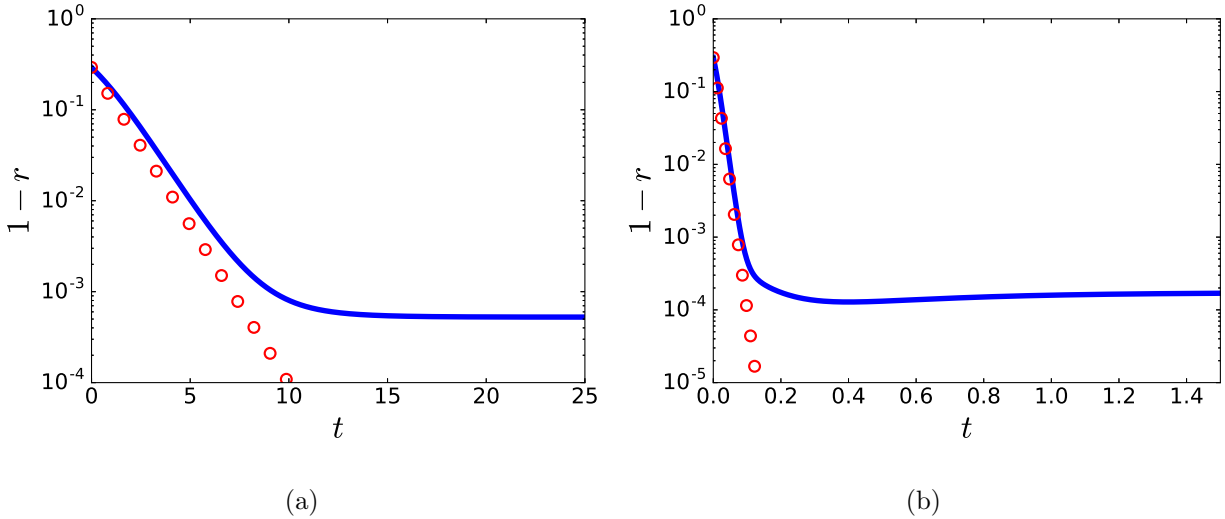


FIG. 9: Time evolution of $1 - r(t)$ and $\eta_r(t)$. The multiplex parameters, symbols and lines are the same as in Fig. 3c and Fig. 3d, except for $\Omega_n^\alpha \in \mathcal{U}(0.8, 1.2)$. (a) Left panel: $\lambda^{12} = 0.1\lambda$ (b) Right panel: $\lambda^{12} = 10.0\lambda$.

V. CONCLUSIONS

We have developed a simple formalism to study the timescales of the global order parameter and the interlayer synchronization of multilayer networks. Our approach has been adapted to a two-layer multiplex with high degrees of synchronization in each layer (i.e. $r_\alpha(t) \approx 1$ for $1 \leq \alpha \leq 2$ and $t \geq 0$), in a particular setup in which nodes are preserved through layers.

We have analyzed the difference between the average phase of each layer of the multiplex network from two different perspectives: spectral analysis and non-linear Kuramoto model. Our analytical results showed that the timescales of the global order parameter τ_r and the interlayer synchronization τ_Δ are inversely proportional to the interlayer coupling strength λ^{12} . Surprisingly, the convergence of the global order parameter is faster than the convergence of interlayer synchronization, and the latter is generally faster than the relaxation time of the multiplex network τ_M . These features do not depend on the specific structures coupled together. Therefore, increasing the interlayer coupling always shortens the global order parameter and the interlayer synchronization transient regimes.

On the other hand, our formalism outlined the effects of frequencies on evolution of the

global order parameter and on interlayer synchronization process. In addition, conditions for an oscillatory behavior were also identified.

The analytical findings were in fairly good agreement with computer simulations. In the case of multiplex networks with relatively small interlayer coupling (i.e. $\lambda^{12} \ll \lambda$), similar average frequencies in each layer (i.e. $\langle \Omega \rangle_1 \approx \langle \Omega \rangle_2$) and high degrees of synchronization in each layer, at the initial time (i.e. $r_\alpha(0) \approx 1$ for $1 \leq \alpha \leq 2$), analytical results and numerical ones were in complete agreement. However, supposing similar average frequencies in each layer, if the interlayer coupling is relatively large (i.e. $\lambda^{12} \gg \lambda$), and there exists an initial intralayer phase heterogeneity (i.e. there is at least one layer G_α that contains two or more oscillators whose phases are different at $t = 0$), numerical results showed deviations from the predicted exponential decay, although major changes of the global order parameter and of the interlayer synchronization were fairly well adjusted by our analytical approach. The timescale of these discrepancies τ_D is inversely proportional to twice the smallest non-zero eigenvalue of the supra-Laplacian matrix \mathcal{L} of the multiplex network, Λ_2 . According to prior works [5, 38], this dependence on Λ_2 implies that deviations from our analytical results are shaped by topological characteristics of the layers involved as well as the respective values of λ and λ^{12} .

When the average frequencies of each layer are dissimilar (i.e. $\langle \Omega \rangle^{12} = \langle \Omega \rangle_1 - \langle \Omega \rangle_2 \neq 0$), computer simulations are in good agreement with our analytical results. If $\Lambda_\Delta \geq |\langle \Omega \rangle^{12}|$, the asymptotic values of the global order parameter and of the interlayer synchronization converge to a non-zero value. If $\Lambda_\Delta \leq |\langle \Omega \rangle^{12}|$, a periodic behaviour is obtained. Discrepancies from our analytical description do not appear, unless the asymptotic values of the global order parameter and of the interlayer synchronization are close to zero (i.e. $\langle \Omega \rangle^{12} \approx 0$).

Thus, under the hypotheses of this work, we conclude that timescale of the global order parameter is at least half times smaller than timescale of multiplex networks (i.e. $2\tau_r \approx 2\tau_D \approx \tau_M = 1/\Lambda_2$) and the major changes of this parameter are fairly well adjusted by our analytical findings (i.e. $\tau_r \approx \tau_\Delta = 1/\Lambda_\Delta = 1/2\lambda^{12}$).

Acknowledgments

This work was supported by the project MTM2015-63914-P from the Ministry of Economy and Competitiveness of Spain and by the Brazilian agency CNPq (grant 305060/2015-

5). RFSA also acknowledges the support of the National Institute of Science and Technology for Complex Systems (INCT-SC Brazil).

APPENDIX: ANALYTICAL RESULTS FOR A MULTIPLEX NETWORK FORMED BY COMPLETE GRAPHS.

A. Eigenvalue spectrum of the supra-Laplacian matrix.

Given an undirected multiplex network \mathcal{M} with $M = 2$ layers, if both layers contain a complete network, then the supra-Laplacian matrix \mathcal{L} has the following eigenvalues Λ :

- (i) $\Lambda = 0$. It is a nondegenerate eigenvalue.
- (ii) $\Lambda = \lambda N$. It is a degenerate eigenvalue. It appears $N - 1$ times.
- (iii) $\Lambda = 2\lambda^{12}$. It is a nondegenerate eigenvalue.
- (iv) $\Lambda = 2\lambda^{12} + \lambda N$. It is a degenerate eigenvalue. It appears $N - 1$ times.

Thus, in case of $\lambda^{12}/\lambda \geq N/2$ ($\lambda^{12}/\lambda < N/2$), the smallest nonzero eigenvalue of the supra-Laplacian matrix is $\Lambda = \lambda N$ ($\Lambda = 2\lambda^{12}$).

B. Estimation of the average time evolution of the linear Kuramoto model.

Given an undirected multiplex network \mathcal{M} with $M = 2$ layers, if both layers contain a complete network, then Eq. 2 results in

$$\dot{\theta}_n^\alpha(t) = \lambda^\alpha N \langle \theta^\alpha \rangle - \lambda^\alpha N \theta_n^\alpha + \lambda^{12} (\theta_n^\beta - \theta_n^\alpha), \quad (25)$$

where

$$\langle \theta^\alpha \rangle = \frac{1}{N} \sum_{x_n^\alpha \in G_\alpha} \theta_n^\alpha. \quad (26)$$

We estimate the average value of $\dot{\theta}_n^\alpha$ in the layer G_α , $\langle \dot{\theta}^\alpha \rangle$. The result is given by

$$\langle \dot{\theta}^\alpha \rangle = \frac{1}{N} \sum_{n=1}^N \dot{\theta}_n^\alpha = -\lambda^{12} (\langle \theta^\alpha \rangle - \langle \theta^\beta \rangle). \quad (27)$$

Note that according to Eq. 27, the sum of the phases of the multiplex network is constant, for $M = 2$, when each layer contains a complete graph, i.e. $\langle \dot{\theta}^1 \rangle + \langle \dot{\theta}^2 \rangle = 0$. Therefore,

$$\langle \theta^1(t) \rangle + \langle \theta^2(t) \rangle = \langle \theta^1(0) \rangle + \langle \theta^2(0) \rangle = \Gamma. \quad (28)$$

On the other hand, according to Eq. 27, it can be written that

$$\langle \dot{\theta}^1 \rangle - \langle \dot{\theta}^2 \rangle = -2\lambda^{12} (\langle \theta^1 \rangle - \langle \theta^2 \rangle). \quad (29)$$

It results in

$$\langle \theta^1(t) \rangle - \langle \theta^2(t) \rangle = (\langle \theta^1(0) \rangle - \langle \theta^2(0) \rangle) e^{-2\lambda^{12}t} = \gamma e^{-2\lambda^{12}t} \quad (30)$$

Hence, the evolution of the average value of θ^1 and of the average value of θ^2 are given by

$$\langle \theta^1(t) \rangle = \frac{\gamma}{2} e^{-2\lambda^{12}t} + \frac{\Gamma}{2}, \quad (31)$$

and

$$\langle \theta^2(t) \rangle = -\frac{\gamma}{2} e^{-2\lambda^{12}t} + \frac{\Gamma}{2}. \quad (32)$$

By considering the series expansion

$$e^{i\theta_n^\alpha} = e^{i\langle \theta^\alpha \rangle} + ie^{i\langle \theta^\alpha \rangle} (\theta_n^\alpha - \langle \theta^\alpha \rangle) - \frac{1}{2} e^{i\langle \theta^\alpha \rangle} (\theta_n^\alpha - \langle \theta^\alpha \rangle)^2 + \dots, \quad (33)$$

we observe that

$$\begin{aligned} \sum_{x_n^\alpha \in G_\alpha} e^{i\theta_n^\alpha} &= N e^{i\langle \theta^\alpha \rangle} + ie^{i\langle \theta^\alpha \rangle} \left(\left[\sum_{x_n^\alpha \in G_\alpha} \theta_n^\alpha \right] - N \langle \theta^\alpha \rangle \right) - \\ &- \frac{1}{2} e^{i\langle \theta^\alpha \rangle} \left(\left[\sum_{x_n^\alpha \in G_\alpha} (\theta_n^\alpha)^2 \right] + N \langle \theta^\alpha \rangle^2 - 2 \langle \theta^\alpha \rangle \sum_{x_n^\alpha \in G_\alpha} \theta_n^\alpha \right) + \dots \approx \\ &\approx N e^{i\langle \theta^\alpha \rangle} - \frac{1}{2} e^{i\langle \theta^\alpha \rangle} (N \langle (\theta^\alpha)^2 \rangle + N \langle \theta^\alpha \rangle^2 - 2N \langle \theta^\alpha \rangle^2) \end{aligned} \quad (34)$$

We characterize the degree of synchronization of each layer G_α by means of its own order parameter, r_α , expressed by

$$r_\alpha(t)e^{i\psi^\alpha(t)} = \frac{1}{N} \sum_{x_n^\alpha \in G_\alpha} e^{i\theta_n^\alpha(t)} \rightarrow r_\alpha(t) = \frac{1}{N} \left| \sum_{x_n^\alpha \in G_\alpha} e^{i\theta_n^\alpha(t)} \right|. \quad (35)$$

Consequently, according to Eq. 34 and Eq. 35, it is straightforward to realize that $\psi^\alpha \approx \langle \theta^\alpha \rangle$ and

$$r_\alpha \approx 1 + \frac{1}{2} \langle \theta^\alpha \rangle^2 - \frac{1}{2} \langle (\theta^\alpha)^2 \rangle. \quad (36)$$

In case $M = 2$, we obtain the following expressions for $\langle (\theta^1)^2 \rangle$, $\langle (\theta^2)^2 \rangle$ and $\langle \theta^1 \theta^2 \rangle$, respectively:

$$\langle (\theta^1)^2 \rangle = \frac{\Gamma^2}{4} + K_1 e^{-2\lambda N t} + \frac{\gamma^2}{4} e^{-4\lambda^{12} t} - K_2 e^{-2(\lambda N + 2\lambda^{12})t} + \frac{\gamma\Gamma}{2} e^{-2\lambda^{12} t} + K_3 e^{-(2\lambda N + 2\lambda^{12})t}, \quad (37)$$

$$\langle (\theta^2)^2 \rangle = \frac{\Gamma^2}{4} + K_1 e^{-2\lambda N t} + \frac{\gamma^2}{4} e^{-4\lambda^{12} t} - K_2 e^{-2(\lambda N + 2\lambda^{12})t} - \frac{\gamma\Gamma}{2} e^{-2\lambda^{12} t} - K_3 e^{-(2\lambda N + 2\lambda^{12})t}, \quad (38)$$

and

$$\langle \theta^1 \theta^2 \rangle = \frac{\Gamma^2}{4} + K_1 e^{-2\lambda N t} - \frac{\gamma^2}{4} e^{-4\lambda^{12} t} + K_2 e^{-2(\lambda N + 2\lambda^{12})t}, \quad (39)$$

where K_1 , K_2 and K_3 are constant values that depend on the initial conditions, given by

$$K_1 = \frac{2 \langle \theta^1 \theta^2 \rangle (0) - \Gamma^2 + \langle (\theta^1)^2 \rangle (0) + \langle (\theta^2)^2 \rangle (0)}{4}, \quad (40)$$

$$K_2 = \frac{2 \langle \theta^1 \theta^2 \rangle (0) + \gamma^2 - \langle (\theta^1)^2 \rangle (0) - \langle (\theta^2)^2 \rangle (0)}{4}, \quad (41)$$

and

$$K_3 = \frac{\langle (\theta^1)^2 \rangle (0) - \langle (\theta^2)^2 \rangle (0) - \gamma\Gamma}{2}. \quad (42)$$

Thus, according to Eq. 31, Eq. 32, Eq. 37 and Eq. 38, the order parameters for layers G_1 and G_2 are given by

$$r_1 \approx 1 - \frac{1}{2} K_1 e^{-2\lambda N t} + \frac{1}{2} K_2 e^{-2(\lambda N + 2\lambda^{12})t} - \frac{1}{2} K_3 e^{-(2\lambda N + 2\lambda^{12})t} = \zeta - \chi, \quad (43)$$

and

$$r_2 \approx 1 - \frac{1}{2}K_1e^{-2\lambda Nt} + \frac{1}{2}K_2e^{-2(\lambda N+2\lambda^{12})t} + \frac{1}{2}K_3e^{-(2\lambda N+2\lambda^{12})t} = \zeta + \chi, \quad (44)$$

where

$$\zeta = \left(e^{2\lambda Nt} - \frac{1}{2}K_1 - \frac{1}{2}K_2e^{-4\lambda^{12}t} \right) e^{-2\lambda Nt}, \quad (45)$$

and

$$\chi = \frac{1}{2}K_3e^{-2\lambda^{12}t}e^{-2\lambda Nt}. \quad (46)$$

Finally, the global order parameter of the multiplex network \mathcal{M} (given by Eq. 7) can be approximated as

$$r = \sqrt{\frac{r_1^2 + r_2^2 + 2r_1r_2 \cos(\Delta)}{4}} \approx \sqrt{\zeta^2 \cos^2\left(\frac{\Delta}{2}\right) + \chi^2 \sin^2\left(\frac{\Delta}{2}\right)}, \quad (47)$$

where

$$\Delta = \psi^1 - \psi^2 \approx \langle \theta^1 \rangle - \langle \theta^2 \rangle = \gamma e^{-2\lambda^{12}t}. \quad (48)$$

-
- [1] Stefano Boccaletti, Ginestra Bianconi, Regino Criado, Charo I Del Genio, Jesus Gómez-Gardeñes, Miguel Romance, Irene Sendiña-Nadal, Zhen Wang, and Massimiliano Zanin. The structure and dynamics of multilayer networks. *Physics Reports*, 544(1):1–122, 2014.
 - [2] M. Kivelä, A. Arenas, M. Barthelemy, J. P. Gleeson, Y. Moreno, and M. A. Porter. Multilayer networks. *J. Complex Netw.*, 2014.
 - [3] Sergey V Buldyrev, Roni Parshani, Gerald Paul, H Eugene Stanley, and Shlomo Havlin. Catastrophic cascade of failures in interdependent networks. *Nature*, 464(7291):1025–1028, 2010.
 - [4] Fan RK Chung. *Spectral graph theory*, volume 92. American Mathematical Soc., 1997.
 - [5] A. Solé-Ribalta, M. De Domenico, N. E. Kouvaris, A. Díaz-Guilera, S. Gómez, and A. Arenas. Spectral properties of the laplacian of multiplex networks. *Phys. Rev. E*, 88:032807, Sep 2013.

- [6] Roni Parshani, Sergey V. Buldyrev, and Shlomo Havlin. Interdependent networks: Reducing the coupling strength leads to a change from a first to second order percolation transition. *Phys. Rev. Lett.*, 105:048701, Jul 2010.
- [7] Jonathan F Donges, Hanna CH Schultz, Norbert Marwan, Yong Zou, and Jürgen Kurths. Investigating the topology of interacting networks. *The European Physical Journal B*, 84(4):635–651, 2011.
- [8] Jianxi Gao, Sergey V Buldyrev, H Eugene Stanley, and Shlomo Havlin. Networks formed from interdependent networks. *Nature Physics*, 8(1):40–48, 2012.
- [9] Federico Battiston, Vincenzo Nicosia, and Vito Latora. Structural measures for multiplex networks. *Phys. Rev. E*, 89:032804, Mar 2014.
- [10] Luis Solá, Miguel Romance, Regino Criado, Julio Flores, Alejandro García del Amo, and Stefano Boccaletti. Eigenvector centrality of nodes in multiplex networks. *Chaos*, 23(3), 2013.
- [11] Manlio De Domenico, Albert Solé-Ribalta, Emanuele Cozzo, Mikko Kivela, Yamir Moreno, Mason A. Porter, Sergio Gómez, and Alex Arenas. Mathematical formulation of multilayer networks. *Phys. Rev. X*, 3:041022, Dec 2013.
- [12] Alessio Cardillo, Jesús Gómez-Gardeñes, Massimiliano Zanin, Miguel Romance, David Papo, Francisco Del Pozo, and Stefano Boccaletti. Emergence of network features from multiplexity. *Sci. Rep.*, 3:1344, 2013.
- [13] Alessio Cardillo, Massimiliano Zanin, Jesús Gómez-Gardeñes, Miguel Romance, Alejandro García del Amo, and Stefano Boccaletti. Modeling the multi-layer nature of the european air transport network: Resilience and passengers re-scheduling under random failures. *Eur. J. Special Topics*, 215(1):23, 2013.
- [14] M. Szell, R. Lambiotte, and S. Thurner. Multirelational organization of large-scale social networks in an online world. *Proc. Natl. Acad. Sci. (USA)*, 107:13636, 2010.
- [15] R. Gallotti and M. Barthelemy. Anatomy and efficiency of urban multimodal mobility. *Sci. Rep.*, 4:6911, 2014.
- [16] R. Gallotti, M. Porter, and M. Barthelemy. Lost in transportation: Information measures and cognitive limits in multilayer navigation. *Science Adv.*, 2:e1500445, 2016.
- [17] Laura Lotero, Rafael Hurtado, Luis Mario Floría, and Jesús Gómez-Gardeñes. Rich do not rise early: spatio-temporal patterns in the mobility networks of different socio-economic classes. *Royal Soc. Open Science*, 3(10):150654, 2016.

- [18] F Radicchi and A Arenas. Abrupt transition in the structural formation of interconnected networks. *Nature Phys.*, 9:717, 2013.
- [19] J. Gómez-Gardeñes, M. De Domenico, G. Gutiérrez, A Arenas, and S. Gómez. Layer-layer competition in multiplex complex networks. *Philos. Trans. Roy. Soc. A*, 373:20150117, 2015.
- [20] Jesús Gómez-Gardeñes, Irene Reinares, Alex Arenas, and Luis Mario Floría. Evolution of cooperation in multiplex networks. *Sci. Rep.*, 2:620, 2012.
- [21] J T. Matamalas, J. Poncela-Casasnovas, and A. Arenas. Strategic incoherence regulates cooperation in social dilemmas on multiplex networks. *Sci. Rep.*, 5:9519, 2015.
- [22] Z. Wang, A. Szolnoki, and M. Perc. Evolution of public cooperation on interdependent networks: The impact of biased utility functions. *EPL*, 97:48001, 2012.
- [23] Z. Wang, L. Wang, and M. Perc. Degree mixing in multilayer networks impedes the evolution of cooperation. *Phys. Rev. E*, 89:052813, 2014.
- [24] F. Sorrentino. Synchronization of hypernetworks of coupled dynamical systems. *New J. Phys.*, 14:033035, 2012.
- [25] L V. Gambuzza, M. Frasca, and J. Gómez-Gardeñes. Intra-layer synchronization in multiplex networks. *EPL*, 110:20010, 2015.
- [26] R. Sevilla-Escoboza, R. Gutiérrez, G. Huerta-Cuellar, S. Boccaletti, J. Gómez-Gardeñes, A. Arenas, and J. M. Buldú. Enhancing the stability of the synchronization of multivariable coupled oscillators. *Phys. Rev. E*, 92:032804, 2015.
- [27] C I. Del Genio, J. Gómez-Gardeñes, I. Bonamassa, and S. Boccaletti. Synchronization in networks with multiple interaction layers. *Science Adv.*, 2:e1601679, 2016.
- [28] Y. Kuramoto. Self-entrainment of a population of coupled non-linear oscillators. In H. Araki, editor, *Lecture Notes in Physics*. Springer Berlin/Heidelberg, 1975.
- [29] Y. Kuramoto. *Chemical Oscillations, Waves, and Turbulence*. Springer Berlin Heidelberg, 1984.
- [30] S. H. Strogatz. *Sync: The Emerging Science of Spontaneous Order*. Hyperion, 2003.
- [31] S. C. Manrubia. *Emergence of Dynamical Order: Synchronization Phenomena in Complex Systems*. WorldScientific, 2004.
- [32] D. Kelly and G. A. Gottwald. On the topology of synchrony optimized networks of a kuramoto-model with non-identical oscillators. *Chaos*, 2011.
- [33] J. A. Acebrón, L. L. Bonilla, C. J. Pérez Vicente, F. Ritort, and R. Spigler. The kuramoto

- model: A simple paradigm for synchronization phenomena. *Rev. Mod. Phys.*, 2005.
- [34] F. A. Rodrigues, T. K. DM. Peron, P. Ji, and J. Kurths. The kuramoto model in complex networks. *Phys. Rep.*, 2016.
- [35] E. Ott and T. M. Antonsen. Low dimensional behavior of large systems of globally coupled oscillators. *Chaos*, 2008.
- [36] E. Barreto, B. Hunt, E. Ott, and P. So. Synchronization in networks of networks: The onset of coherent collective behavior in systems of interacting populations of heterogeneous oscillators. *Phys. Rev. E*, 2008.
- [37] D. Anderson, A. Tenzer, G. Barlev, M. Girvan, T. M. Antonsen, and E. Ott. Multiscale dynamics in communities of phase oscillators. *Chaos*, 2012.
- [38] Sergio Gomez, Albert Diaz-Guilera, Jesus Gomez-Gardeñes, Conrad J Perez-Vicente, Yamir Moreno, and Alex Arenas. Diffusion dynamics on multiplex networks. *Physical Review Letters*, 110(2):028701, 2013.
- [39] M. De Domenico, M. A. Porter, and A. Arenas. Muxviz: a tool for multilayer analysis and visualization of networks. *J. Complex Networks*, 2015.
- [40] A. B. Serrano, J. Gómez-Gardeñes, and R. F. S. Andrade. Optimizing diffusion in multiplexes by maximizing layer dissimilarity. *Phys. Rev. E*, 2017.
- [41] K.M. Lee, B. Min, and K.I. Goh. Towards real-world complexity: an introduction to multiplex networks. *Eur. Phys. J. B*, 2015.
- [42] M. De Domenico, C. Granell, M A. Porter, and A. Arenas. The physics of spreading processes in multilayer networks. *Nature Phys.*, 12:901, 2016.
- [43] A. Arenas, A. Díaz-Guilera, and C. J. Pérez-Vicente. Synchronization reveals topological scales in complex networks. *Phys. Rev. Lett.*, 2006.
- [44] A. Arenas, A. Díaz-Guilera, and C. J. Pérez-Vicente. Synchronization processes in complex networks. *Physica D*, 2006.
- [45] J. A. Almendral and A. Díaz-Guilera. Dynamical and spectral properties of complex networks. *New Journal of Physics*, 2007.
- [46] C. Grabow, S. Grosskinsky, and M. Timme. Speed of complex network synchronization. *Eur. Phys. J. B*, 2011.
- [47] C. Grabow, S. Hill, S. Grosskinsky, and M. Timme. Do small worlds synchronize fastest? *Europhysics Letters*, 2010.

- [48] S.-W. Son, H. Jeong, and H. Hong. Relaxation of synchronization on complex networks. *Physical Review E*, 2008.
- [49] V. Avalos-Gaytán, J. A. Almendral, D. Papo, S. E. Schaeffer, and S. Boccaletti. Assortative and modular networks are shaped by adaptive synchronization processes. *Phys. Rev. E*, 2012.